Physisorption-like Interaction at the Interfaces Formed by Pentacene and Samarium

N. Koch,*,† J. Ghijsen,‡ R. L. Johnson,§ J. Schwartz,⊥ J.-J. Pireaux,‡ and A. Kahn†

Department of Electrical Engineering, Princeton University, Princeton, New Jersey 08544, Laboratoire Interdisciplinaire de Spectroscopie Electronique, Facultés Universitaires Notre-Dame de la Paix, B-5000 Namur, Belgium, II. Institut für Experimentalphysik, Universität Hamburg, D-22761 Hamburg, Germany, and Department of Chemistry, Princeton University, Princeton, New Jersey 08544

Received: September 20, 2001; In Final Form: February 4, 2002

We have investigated the nature of the interaction between samarium (Sm) and pentacene, and the energy level alignment at the resulting interfaces. The valence electronic structure of in situ prepared samples, i.e., pentacene evaporated onto Sm surfaces and vice versa, was investigated with ultraviolet photoelectron spectroscopy. Pentacene appears to physisorb on the metal surface. Sm also appears to interact weakly when evaporated on the organic material, forming clusters at low coverage. Indications of a valence change of Sm upon evolution from clusters to metallic film are found. The highest occupied molecular orbital of pentacene is measured at 1.8_5 eV below the metal Fermi level E_F for both evaporation sequences. Estimating the energy of the lowest unoccupied molecular orbital of pentacene using the transport gap, we obtain a barrier of only 0.3_5 eV for the injection of electrons from the metal into the organic material.

Introduction

Conjugated organic systems constitute one of the most promising classes of materials for novel electronic and optoelectronic applications.[1−7] Pentacene in particular has attracted considerable attention since it was shown to exhibit structural and electronic properties that have been successfully used in high-performance devices, i.e., field effect transistors.[8−11] The chemical and electrical properties of interfaces of organic compounds determine to a large extent charge carrier injection and device stability, and are thus exceedingly important for device performance. Yet little information is presently available in the literature on pentacene interfaces, in particular with metals that could be used for carrier injection. We begin to address this issue by investigating the interaction between pentacene and a low work function metal. Numerous studies of interfaces between conjugated organic materials and low work function metals, such as alkali and alkaline-earth metals, have demonstrated that strong chemical interactions can take place between metal atoms and organic molecules.[12−22] These reactions, which are sometimes accompanied by substantial diffusion,[23] are often unwanted, as they change the expected interface properties.

Samarium (Sm) is chosen for the present study because of its low work function (ca. 2.7 eV [24]), which is comparable to the pentacene electron affinity (EA) (ca. 2.7 eV [25]). This makes it a good candidate for forming an efficient electron injection contact. Sm has also been found to interact weakly with another conjugated organic molecule (*p*-sexiphenyl),[26] in stark contrast to the charge-transfer reactions occurring with metals of similar low work function (Ca, alkali metals).[20−22] We use ultraviolet photoelectron spectroscopy (UPS) to investigate the valence electronic structure of pentacene (i) as it is deposited onto the metallic surface of Sm and (ii) as it changes upon deposition of Sm atoms/clusters from the vapor phase. Samples are prepared and measured under ultrahigh vacuum (UHV) conditions, and the organic material and metal, respectively, are evaporated in incremental small steps until the interface formation process is complete, as judged by UPS.

Experimental Section

The photoemission experiments are done on the FLIPPER II beamline in Hasylab at DESY[27] in an ultrahigh vacuum (UHV) system consisting of a preparation−evaporation chamber (base pressure 2×10^{-10} mbar) and an analysis chamber (base pressure 1×10^{-10} mbar). The evaporations of pentacene and Sm are performed in situ, at pressures of about 5×10^{-9} mbar for pentacene and 2×10^{-9} mbar for Sm. Pentacene (purchased from Aldrich Chem. Co.) is evaporated from a resistively heated pinhole source, while Sm is evaporated from a Knudsen-type cell. In situ sputtered gold films on silicon oxide (prepared ex situ) are used to determine the position of the Fermi level and the resolution of the electron spectrometer (ca. 0.15 eV width of the intensity drop from 80% to 20% on the Au Fermi edge). Au/SiO_2 also serves as substrate for the deposition of the Sm films. The rates of deposition of the pentacene (bulk density 1.33 g/cm^3 [28]) and Sm (bulk density 7.54 g/cm^3) overlayers are monitored with a quartz microbalance. No correction is made for possible differences in sticking coefficient between the microbalance and the actual sample. The materials are evaporated in a stepwise manner, with very small initial coverages. Following each incremental deposition, the samples are transferred under UHV to the analysis chamber. The secondary electron cutoff is recorded with the sample biased negatively with respect to the electron spectrometer. The energy positions of the cutoff and of the top of the highest occupied molecular orbital (HOMO) are determined by linear extrapolation to the background. The vacuum level of the surface is obtained by adding the photon energy to the cutoff energy.[29] The ionization energy (IE) of the sample (equal to the work function in the case of the metallic surface) is therefore obtained at each stage of the experiment as the difference between the incident photon

† Department of Electrical Engineering, Princeton University.
‡ Facultés Universitaires Notre-Dame de la Paix.
§ Universität Hamburg.
⊥ Department of Chemistry, Princeton University.

10.1021/jp0135813 CCC: $22.00
Published on Web 03/30/2002

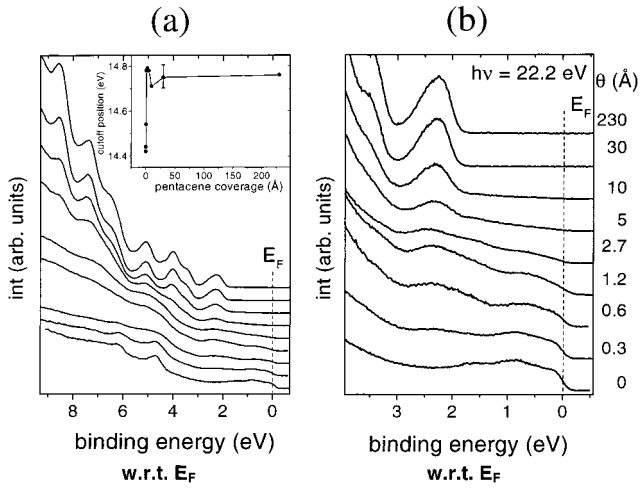

Figure 1. Survey (a) and near E_F region (b) photoemission spectra for increasing pentacene coverage (θ) on Sm. Inset: kinetic energy position of the secondary electron cutoff.

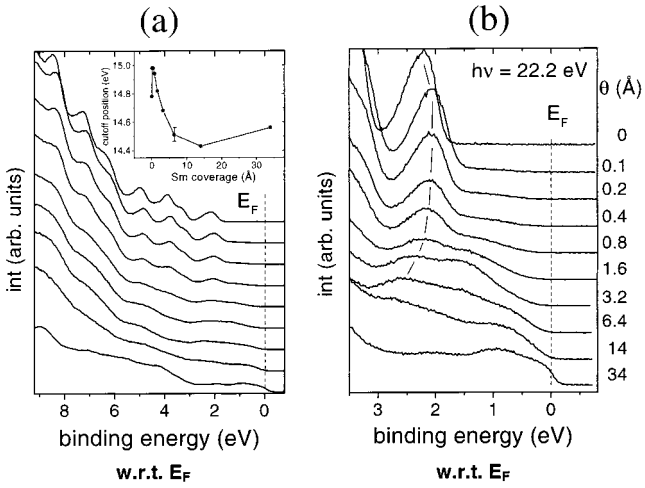

Figure 2. Survey (a) and near E_F region (b) photoemission spectra for increasing Sm coverage (θ) on pentacene. Inset: kinetic energy position of the secondary electron cutoff.

energy and the total width of the energy distribution curve. We estimate the error in energy determination to be smaller than ±0.1 eV. Photon energies of 22.2 and 40.2 eV are used in order to vary the relative photoemission cross sections of pentacene and Sm derived spectral features.

Results

Pentacene on Samarium. A 90 Å thick film of samarium is deposited onto the Au/silicon oxide substrate. The photoemission spectrum of this film (lowest curve in Figure 1a) resembles that of metallic Sm.[26] The features at 4.8 and 6.3 eV binding energies (BE) are associated with bulk Sm, and the work function of the metallic surface is 2.7 eV. Increasing amounts of pentacene are subsequently deposited onto the Sm. The survey spectra of the valence states and a closeup of the energy region near the Fermi energy E_F are shown in Figure 1a and Figure 1b, respectively. All spectra are obtained with an incident photon energy of 22.2 eV. The nominal thickness of the pentacene layer is given on the right side of the figure. The survey spectra show that small amounts of pentacene effectively attenuate the Sm emission and that distinct emission features of the organic material become evident from 5 Å coverage onward. The closeup spectra of Figure 1b show that the first evaporation step (0.3 Å) already produces a new photoemission feature at a BE of ∼2.3 eV. As more pentacene is deposited, this feature grows in intensity at constant BE, and finally is identified as the emission from the pentacene HOMO.[30] Conversely, the photoemission features from the metallic Sm substrate are eliminated for coverages of 30 Å and above, leaving the energy-gap region of pentacene (above the HOMO) free of valence features. The onset of the HOMO is found at 1.8_5 eV below E_F. The change in the sample work function, monitored by the shift of the secondary electron cutoff, is shown as inset in Figure 1a. For increasing pentacene coverage, the onset moves abruptly toward higher kinetic energy and stabilizes (within experimental error) ca. 0.3_5 eV above the initial value for a pentacene thickness of 5 Å. The final sample work function is 3.0_5 eV, and the ionization potential of pentacene is 4.9 eV. Virtually identical experimental results are obtained for another deposition sequence of pentacene on Sm with a photon energy of 40.2 eV.

Samarium on Pentacene. The starting substrate for the deposition of Sm onto the organic compound is a 230 Å thick pentacene film grown on Sm. The survey photoemission spectra of this series are shown in Figure 2a, and the low BE region is shown in greater detail in Figure 2b. Spectra were recorded with a photon energy of 22.2 eV. Following the evaporation of only 0.1 Å Sm, the whole photoemission spectrum shifts rigidly toward *lower* BE by 0.2 eV. No change in the line shape of the pentacene emission peaks can be perceived, except for a weak broad emission that appears in the energy gap of the organic material (discernible from the pentacene HOMO onset and ranging to ca. 0.3 eV below the Fermi level). Subsequent Sm depositions lead to an attenuation of the pentacene emission and an intensity increase in the new emission close to E_F. The line shape of the pentacene emission does not change noticeably and all features appear to shift rigidly toward *higher* BE, as indicated by the lines drawn for the HOMO in Figure 2b. At a Sm coverage of 6.4 Å, the HOMO can still be identified, and is centered at 2.5 eV (compared to 2.2 eV for the pristine film and 2.0 eV with 0.1 Å Sm). As the coverage increases, the center of gravity of the new intragap emission moves closer to E_F. At 14 Å Sm coverage the whole spectrum hardly resembles that of pentacene. At 34 Å, a Fermi edge is clearly visible, and the spectrum can be identified as that of Sm metal.

The movement of the secondary electron cutoff for this deposition sequence is shown in the inset in Figure 2a. An initial 0.2 eV shift toward higher kinetic energy, equal to that of the valence electronic region, is detected, followed by a progressive decrease in kinetic energy. The work function is 3.0_5 eV for the pristine pentacene film, 3.2_5 eV after the deposition of 0.1 Å Sm, and 2.8 eV for the metallic Sm film. A similar study repeated on another sample using an incident photon energy of 40.2 eV led to equivalent results.

Discussion

Pentacene on Samarium. The photoemission feature that appears to be the HOMO of pentacene in Figure 1b (at 2.3 eV binding energy) has a constant BE throughout the deposition sequence. Close inspection of deeper lying molecular orbitals (from Figure 1a) shows that these levels do not shift, either. The absence of bonding-related shifts is a strong indication of a weak interaction between metal substrate and organic overlayer. The formation of interfacial covalent bonds would result in a substantial changes in the BE and line shape of molecular orbitals (MOs),[19,31−33] especially those of purely π-derived MOs such as the HOMO. This type of interaction can therefore be ruled out here. The low work function of Sm also leads us to

expect an electron transfer from the metal to the pentacene, as is the case for many low work function metal−conjugated organic molecular systems.[12−22] Such a charge transfer (often referred to as "doping") should result in a significant change in the electronic structure of the molecule. This change is generally observed as a destabilization of the HOMO and the appearance of a new photoemission feature close to E_F due to the filling of the LUMO of the pristine molecule with electrons.[34] In our experiment, we observe a photoemission feature above the HOMO, but it is attributed to the substrate only. In a separate experiment[35] we have deposited Rb onto pentacene films. As expected for an alkali metal, charge transfer takes place, and the photoemission spectrum changes dramatically from pristine to doped pentacene. The absence of a similar change in the near E_F energy region and bonding shifts of deeper lying MOs in the present experiment lead us to conclude that the interaction of pentacene with the Sm is mainly physisorptive. Analogous observations were made for *p*-sexiphenyl on Sm surfaces,[26] for which the attenuation and line shape change of the metal substrate valence emission close to E_F progress in a similar manner.

The UPS data show the Fermi level of the metal 1.8_5 eV above the HOMO onset of pentacene. This value is almost equal to the optical energy gap of 1.88 eV,[28] and it is very close to the charge-transport gap of pentacene of 2.2 eV.[25,28] The common practice in the literature has been to add the optical energy gap to the HOMO binding energy to estimate the electron injection barrier, yielding in the present case a value close to zero. However, the more accurate procedure is to use the charge-transport gap, which results in an injection barrier for electrons from Sm into pentacene of 0.3_5 eV, still an appreciably small value.

From the evolution of the intensity of the pentacene-derived photoemission features, some conclusions on the growth mode of the organic molecules on Sm can be drawn. An almost complete attenuation of the substrate emission above the HOMO occurs between 5 and 10 Å of pentacene. For pentacene molecules standing with their long molecular axis perpendicular to the substrate surface, this range of coverage corresponds to 1/3 to 2/3 of one monolayer (the length of one pentacene molecule is ca. 16 Å [36]). Since such a low coverage is incompatible with the strong attenuation of the substrate signal, we suggest that the molecules are oriented with their long molecular axis parallel to the metal surface. The idea that a complete monolayer is formed around a nominal coverage of 5 Å is supported by the fact that the increase in sample work function also saturates near this film thickness (see inset in Figure 1a). This finding is in line with reports on the orientation of pentacene and related conjugated molecules on other clean metal surfaces.[37−40]

Samarium on Pentacene. The spectral evolution for incremental Sm deposition on pentacene is not a simple reversal of that of the previous case. In particular, the initial shift of the pentacene features to lower BE followed by a progressive shift to higher BE for subsequent Sm depositions (Figure 2) do not have a straightforward explanation. To obtain a better insight into the mechanism(s) responsible for these shifts, we plot the same spectra on a BE scale corrected for the changes in sample work function, i.e., with respect to the vacuum level set at zero (Figure 3). The position of E_F is indicated for each curve by a vertical bar. Within experimental error, there is no shift of the pentacene HOMO for all Sm coverages on this BE scale. The Sm-related emission intensity increases and its spectral weight

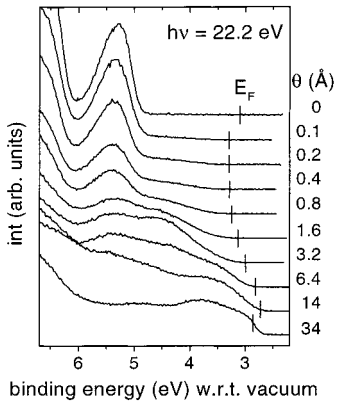

Figure 3. Photoemission spectra for increasing Sm coverage (θ) on pentacene on a binding energy scale relative to the vacuum level, set to zero. The position of E_F is indicated with a bar on each spectrum.

moves toward smaller BE. After the initial shift of the sample work function from 3.0_5 to 3.2_5 eV, it gradually shifts to lower values, to reach its minimum of 2.7_0 eV at a nominal Sm coverage of 14 Å. The last evaporation step results in a metallic Sm film with a work function of 2.8_0 eV.

These experimental observations can be explained in the following way. The fact that the binding energy of the pentacene features remains constant with respect to the vacuum level as a function of Sm deposition suggests that the molecules do not undergo significant chemical changes. The interaction between the organic material and the metal atoms is weak. We propose that the E_F movement, caused by Sm deposition, is due to states induced by the adatoms. The first Sm evaporation produces small clusters or islands of Sm atoms on the organic surface. These aggregates of a few atoms are presumably semiconducting. Their electronic structure, i.e., the binding energy of occupied and empty electronic states, is strongly, although not monotonically, dependent on the number and geometry of their constituent atoms.[41−43] The position of E_F at the organic surface following the first Sm deposition is therefore a consequence of the introduction of a new density of occupied and unoccupied states on the surface of the organic film. However, at present a detailed explanation for this initial shift of E_F toward *higher* BE in Figure 3 cannot be given, as the exact size distribution and geometry of the clusters is unknown. Subsequent depositions of Sm increase the average size of the aggregates and reduce their energy gap. The BE of the highest occupied states of the clusters is reduced,[42] the movement of E_F is inverted (in Figure 3), and the pentacene features shift to higher BE (in Figure 2b). The emission intensity from Sm close to the Fermi level increases. At 14 Å coverage, no photoelectrons at E_F are detected, indicating that there are no large metallic Sm aggregates on the surface. (We can rule out significant diffusion of Sm into the pentacene bulk, as the attenuation of the pentacene photoemission features at a nominal coverage of 3.2 Å (ca. 1 monolayer of Sm) is already very strong.) Provided that Sm does not grow in a layer by layer mode on pentacene, this is not totally surprising, as 14 Å Sm would correspond to less than 4 close packed monolayers,[24] allowing for the formation of clusters with dimensions smaller than those required to develop metallicity. With the radius of one Sm atom being 1.8 Å,[44] we can estimate the average number of atoms per cluster at such a coverage to be smaller than 100. Only after the final evaporation step is a true metallic Sm film formed. Similar experimental observations have been reported for a number of metals deposited on insulating or semiconducting substrates.[41,42,45−47]

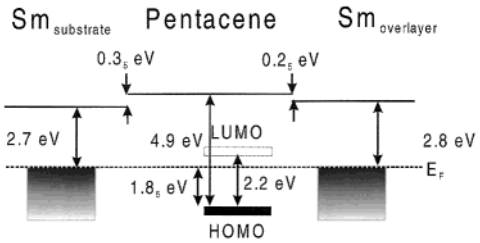

Figure 4. Schematic energy level diagram of the sandwich structure Sm/pentacene/Sm derived from photoemission experiments.

The somewhat unexpected 0.1 eV increase in sample work function from 14 to 34 Å might indicate a change in the Sm valence when going from the Sm clusters to the metal. A similar behavior of sample work function has been observed for the growth of Sm on Ta.[48] It is known that the valence of Sm in a film differs for bulk (trivalent, $4f^5(5d\ 6s)^3$) and surface (mixed trivalent and divalent, $4f^6(5d\ 6s)^2$),[49,50] and thus might differ as well for clusters. Indeed, an increase in the ionization potential (and work function of the metal) for Sm clusters is predicted theoretically[43] when going from a valence of 3 to a valence of 2. The difference in the work function of our final metal film (2.8_0 eV) and the Sm film on Au (2.7_0 eV) is attributed to different surface morphologies of the two films,[51,52] which is very likely because the "substrates" (pentacene vs gold) are very different in nature as well.

Finally, we are able to draw a schematic energy level diagram of the investigated metal/organic semiconductor/metal structure, depicted in Figure 4. Given are the measured metal work functions and the binding energy of the pentacene HOMO onset. The value for the LUMO is calculated by adding the charge-transfer gap[28] to the HOMO binding energy. One can see that on both sides of the sandwich structure the metal Fermi level is 0.3_5 eV below the LUMO, making electron injection into the organic material very favorable. The van der Waals type interaction at the present interfaces does not allow for a strong perturbation of the electronic states of the two materials. Thus, basically a "vacuum level alignment" prevails, except that there is a small interface dipole measured (ca. 0.3 eV; see Figure 4) from the secondary electron cutoff in UPS. The origin of this change in the sample vacuum level is most likely a consequence of a change in the Sm metal surface dipole induced by the molecular adsorbate.[53,54] The difference in the vacuum level offsets of 0.1 eV on the two sides is a consequence of the different metal work functions.

Conclusions

Despite the low work function of samarium, we have observed evidence for a weak interaction (physisorption) between both Sm metal and Sm clusters and pentacene. Independent of the deposition sequence, the energy level alignment at these interfaces was found to be very favorable for the injection of electrons from the metal into the organic semiconductor. The pentacene HOMO is 1.8_5 eV below the Sm Fermi level, leading to an electron injection barrier estimated at 0.3_5 eV. The evolution of the photoemission line shape near E_F and the concomitant change in the sample work function indicate that Sm grows in the form of clusters on the organic surface. A change in the Sm atom valence state is proposed when the overlayer evolves from clusters (trivalent) to metal (divalent on the surface).

Acknowledgment. The authors thank Dr. Chongfei Shen and Dr. Jens Pflaum for stimulating discussions. This work was supported by IHP-Contract HPRI-CT-1999-00040 of the European Commission. Part of this work was supported by a grant of the NSF (DMR-0097133) and by the MRSEC program of the NSF (DMR-98-09483). We acknowledge the financial support of the Interuniversity Research Projects (PAI/IUA) on "Sciences of Interfacial and Mesoscopic Structures" sponsored by the Belgian Prime Minister's Office (Federal Services for Scientific, Technical and Cultural Affairs). R.L.J. acknowledges financial support from the Bundesministerium fuer Bildung, Wissenschaft, Forschung und Technologie (BMBF) Project No. 05 KS1GUC/3. J.G. acknowledges support by the NFSR (Belgium).

References and Notes

(1) Tang, C. W.; Slyke, S. A. v. *Appl. Phys. Lett.* **1987**, *51*, 913.
(2) Burroughes, J. H.; Bradley, D. D. C.; Brown, A. R.; Marks, R. N.; Mackey, K.; Friend, R. H.; Burns, P. L.; Holmes, A. B. *Nature* **1990**, *347*, 539.
(3) Braun, D.; Heeger, A. J. *Appl. Phys. Lett.* **1991**, *58*, 1982.
(4) Bulovic, V.; Gu, G.; Burrows, P. E.; Forrest, S. R.; Thompson, M. E. *Nature* **1996**, *380*, 29.
(5) Sariciftci, N. S.; Smilowitz, L.; Heeger, A. J.; Wudl, F. *Science* **1992**, *258*, 1474.
(6) Granstrom, M.; Petritsch, K.; Arias, A. C.; Lux, A.; Andersson, M. R.; Friend, R. H. *Nature* **1998**, *385*, 257.
(7) Schön, J. H.; Dodabalapur, A.; Kloc, C.; Batlogg, B. *Science* **2000**, *290*, 963.
(8) Dimitrakopoulos, C. D.; Brown, A. R.; Pomp, A. *J. Appl. Phys.* **1996**, *80*, 2501.
(9) Schön, J. H.; Berg, S.; Kloc, C.; Batlogg, B. *Science* **2000**, *287*, 1022.
(10) Schön, J. H.; Kloc, C.; Batlogg, B. *Appl. Phys. Lett.* **2000**, *77*, 2473.
(11) Gundlach, D. J.; Lin, Y. Y.; Jackson, T. N.; Nelson, S. F.; Schlom, D. G. *IEEE Electron. Device Lett.* **1997**, *18*, 87.
(12) Ramsey, M. G.; Schatzmayr, M.; Stafstrom, S.; Netzer, F. P. *Europhys. Lett.* **1994**, *28*, 85.
(13) Ramsey, M. G.; Steinmuller, D.; Netzer, F. P. *Phys. Rev. B* **1990**, *42*, 5902.
(14) Fahlman, M.; Beljonne, D.; Logdlund, M.; Friend, R. H.; Holmes, A. B.; Bredas, J. L.; Salaneck, W. R. *Chem. Phys. Lett.* **1993**, *214*, 327.
(15) Logdlund, M.; Dannetun, P.; Fredriksson, C.; Salaneck, W. R.; Bredas, J. L. *Phys. Rev. B* **1996**, *53*, 16327.
(16) Rajagopal, A.; Kahn, A. *J. Appl. Phys.* **1998**, *84*, 355.
(17) Johansson, N.; Osada, T.; Stafstrom, S.; Salaneck, W. R.; Parente, V.; dos Santos, D. A.; Crispin, X.; Bredas, J. L. *J. Chem. Phys.* **1999**, *111*, 2157.
(18) Greczynski, G.; Fahlman, M.; Salaneck, W. R. *J. Chem. Phys.* **2000**, *113*, 2407.
(19) Shen, C.; Kahn, A.; Schwartz, J. *J. Appl. Phys.* **2001**, *89*, 449.
(20) Koch, N.; Leising, G.; Yu, L. M.; Rajagopal, A.; Pireaux, J. J.; Johnson, R. L. *J. Vac. Sci. Technol., A: Vac. Surf. Films* **2000**, *18*, 295.
(21) Koch, N.; Rajagopal, A.; Ghijsen, J.; Johnson, R. L.; Leising, G.; Pireaux, J. J. *J. Phys. Chem. B* **2000**, *104*, 1434.
(22) Koch, N.; Oji, H.; Ito, E.; Zojer, E.; Ishii, H.; Leising, G.; Seki, K. *Appl. Surf. Sci.* **2001**, *175*, 764.
(23) Parthasarathy, G.; Shen, C.; Kahn, A.; Forrest, S. R. *J. Appl. Phys.* **2001**, *89*, 4986.
(24) *CRC Handbook of Chemistry and Physics*; Lide, D. R., Fredrikse, H. P. R., Eds.; CRC Press: London, 1995.
(25) Gao, W. Private communication.
(26) Koch, N.; Zojer, E.; Rajagopal, A.; Ghijsen, J.; Johnson, R. L.; Leising, G.; Pireaux, J. J. *Adv. Funct. Mater.* **2001**, *11*, 51.
(27) Johnson, R. L.; Reichardt, J. *Nucl. Instrum. Methods* **1983**, *208*, 719.
(28) Silinsh, E. A. *Organic Molecular Crystals*; Springer: Berlin, 1980; Vol. 16.
(29) Hill, I. G.; Rajagopal, A.; Kahn, A. *J. Appl. Phys.* **1998**, *84*, 3236.
(30) Ozaki, H. *J. Chem. Phys.* **2000**, *113*, 6361.
(31) Dannetun, P.; Lögdlund, M.; Fredriksson, C.; Lazzaroni, R.; Fauquet, C.; Stafström, S.; Spangler, C. W.; Brédas, J.-L.; Salaneck, W. R. *J. Chem. Phys.* **1994**, *100*, 6765.
(32) Salaneck, W. R.; Stafström, S.; Brédas, J.-L. *Conjugated polymer surfaces and interfaces; electronic and chemical structure of interfaces for polymer light emitting devices*; Cambridge University Press: Cambridge, 1996.
(33) Rajagopal, A.; Koch, N.; Ghijsen, J.; Johnson, R. L.; Kaeriyama, K.; Leising, G.; Pireaux, J. J. *J. Appl. Phys.* **2000**, *87*, 1331.
(34) Salaneck, W. R.; Brédas, J.-L. *Synth. Met.* **1994**, *67*, 15.

(35) Koch, N.; Ghijsen, J.; Ruiz, R.; Pflaum, J.; Johnson, R. L.; Pireaux, J.-J.; Schwartz, J.; Kahn, A. *Mater. Res. Soc. Symp. Proc.* **2002**, *708*, BB.2.4.1.

(36) Campbell, R. B.; Trotter, J.; Robertson, J. M. *Acta Crystallogr.* **1961**, *14*, 705.

(37) Schuerlein, T. J.; Schmidt, A.; Lee, P. A.; Nebesny, K. W.; Armstrong, N. R. *Jpn. J. Appl. Phys. Part 1: Regul. Pap. Short Notes Rev. Pap.* **1995**, *34*, 3837.

(38) Oji, H.; Ito, E.; Furuta, M.; Kajikawa, K.; Ishii, H.; Ouchi, Y.; Seki, K. *J. Electron Spectrosc. Relat. Phenom.* **1999**, *101*−*103*, 517.

(39) Onoda, M.; Tada, K.; Nakayama, H. *J. Appl. Phys.* **1999**, *86*, 2110.

(40) Koch, N.; Hosoi, Y.; Ishii, H.; Vollmer, A.; Leising, G.; Seki, K. *Mater. Res. Soc. Symp. Proc.* **2000**, *598*, BB.11.13.1.

(41) Hu, Y.; Wagener, T. J.; Gao, Y.; Meyer, H. M., III; Weaver, J. H. *Phys. Rev. B* **1988**, *38*, 3037.

(42) Eberhardt, W.; Fayet, P.; Cox, D. M.; Fu, Z.; Kaldor, A.; Sherwood, R.; Sondericker, D. *Phys. Rev. Lett.* **1990**, *64*, 780.

(43) Durakiewicz, T.; Halas, S. *Chem. Phys. Lett.* **2001**, *341*, 195.

(44) Kittel, C. *Introduction to Solid State Physics*, 4th ed.; Wiley: New York, 1971.

(45) Colbert, J.; Zangwill, A.; Strongin, M.; Krummacher, S. *Phys. Rev. B* **1983**, *27*, 1378.

(46) Mason, M. G. *Phys. Rev. B* **1983**, *27*, 748.

(47) Sakho, O.; Sacchi, M.; Sirotti, F.; Rossi, G. *Phys. Rev. B* **1993**, *47*, 3797.

(48) Strisland, F.; Raaen, S.; Ramstad, A.; Berg, C. *Phys. Rev. B* **1997**, *55*, 1391.

(49) Wertheim, G. K.; Crecelius, G. *Phys. Rev. B* **1978**, *40*, 813.

(50) Tao, L.; Goering, E.; Horn, S.; Denboer, M. L. *Phys. Rev. B* **1993**, *48*, 15289.

(51) Cardona, M.; Ley, L. In *Photoemission in Solids I*; Topics in Applied Physics 26; Cardona, M., Ley, L., Eds.; Springer: Berlin, 1978; p 16.

(52) Niemantsverdriet, J. W. *Spectroscopy in Catalysis: an introduction*; VCH-Verlagsgesellschaft: Weinheim, 1993.

(53) Ishii, H.; Sugiyama, K.; Ito, E.; Seki, K. *Adv. Mater.* **1999**, *11*, 605.

(54) Koch, N.; Rajagopal, A.; Leising, G.; Pireaux, J.-J. Organic-Metal Interfaces: From Physisorption to Covalent Bonding. In *Conjugated Polymer and Molecular Interfaces: Science and Technology for Photonic and Optoelectronic Applications*; Salaneck, W. R., Seki, K., Kahn, A., Pireaux, J.-J., Eds.; Marcel Dekker: New York, 2001; p 205.